Resolving and Contextualizing the Signal of Greenland Ice Loss 2014–2017

Benjamin Getraer

A Junior Paper
Presented to the Faculty
of Princeton University
in Candidacy for the Degree
of Bachelor of Arts

Recommended for Acceptance
by the Department of
Geosciences
Adviser: Frederik J. Simons
Second Reader: Jessica Irving

March 9, 2018

This paper represents my own work in accordance with University regulations,

Benjamin Getraer

Abstract

The immediate future of Earth's climate hinges in part on the response of frozen water on Earth's surface to increasing mean global temperature. Our detection and understanding of the mass variations of Earth's ice caps and glaciers have been revolutionized by the time-variable global geopotential data products from the Gravity Recovery and Climate Experiment (GRACE) satellite mission. Prior work with the GRACE record revealed a significant departure in 2013–2014 from the previously quadratic downward trend of Greenland ice mass. We use Slepian functions (linear combinations of spherical harmonic functions) to optimally capture geographically localized target signals present in the GRACE time series, model monthly mass change on Greenland over the complete GRACE record, and compare the residuals to forcing from the North Atlantic Oscillation. We find that a linear, rather than quadratic, trend of -239 Gt per year best describes Greenland mass change over the completed GRACE record, and that the 2013–2014 deviations from the linear trend may be associated with irregular atmospheric forcing at the surface.

Key Points:

1. We use geopotential data products from the completed GRACE mission.
2. We model the geopotential field in time over Greenland using spherical Slepian functions.
3. We find a linear trend of Greenland mass loss.
4. We compare inter-annual variability of the Greenland ice loss trend to forcing from the North Atlantic Oscillation.

Acknowledgements

Thank you to my adviser Prof. Frederik J. Simons who helped me with the conceptualization, direction, and revision of this project, to my second reader Prof. Jessica Irving for feedback, suggestions, and encouragement, to Dr. Amanda Irwin Wilkins and "The Hare" writing workshop group for discussing and editing various figures and drafts. Thank you to Prof. Adam C. Maloof who taught me LaTeX, and to Dr. Chris Harig for providing some of the data files.

Contents

List of Figures

Introduction

Over the past century, average global surface temperature has been rising at an increasing rate, with a total increase of about 0.75° C between 1850 and 2012 (Hartmann et al., 2013).Warming has contributed to a widely observed reduction in the mass of the cryosphere, including sea ice and temperate glaciers (approximately −4% per decade and −300 Gt per year, respectively; Vaughan et al., 2013), as well as the Greenland and Antarctic ice sheets (approximately−244 Gt and −92 Gt per year, respectively; Harig & Simons, 2015, 2016). Massive loss of ice has significant repercussions for human civilization because it is raising sea level at increasing rates — about 1–2 mm per year at the end of the last decade (Vaughan et al., 2013). The Greenland ice-sheet covers just over 1% of Earth's surface, and if completely melted would raise sea level by over 7 m (Vaughan et al., 2013). Determining the expected rate and acceleration of ice melt into the near future is essential to understanding and addressing the changing conditions of the planet.

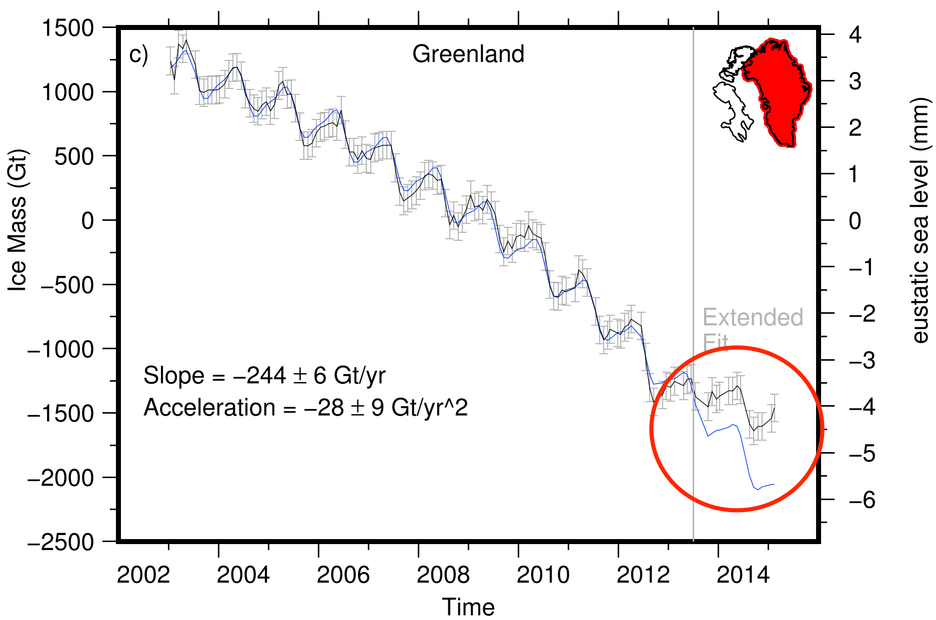

Figure 1: Total ice mass changes calculated using GRACE RL05 data products and a Slepian basis for Greenland (see Data and Methods: Methods of GRACE Data Reduction), adapted from Harig & Simons (2016), their Figure 4. Shown is the variation of the GRACE observations (black) from the modeled trend (blue) — note the significant departure of the 2014 GRACE observations from the extrapolated trend of the previous decade (circled in red). Error-bars represent 2σ based on the combined variance of Slepian coefficients f_α (see Data and Methods: The Slepian Basis).

On a continental scale, mass change from ice loss has been detected and mapped using measured changes in Earth's gravitational potential (geopotential) field. Geopotential measurements from the NASA Gravity Recovery and Climate Experiment (GRACE) satellites have been publicly available since the launch of the mission in 2002, and have greatly improved our understanding of mass change in expansive and remote regions such as the continental ice caps.

Previous studies have modeled ice mass on the Greenland ice-sheet using gravimetric methods such as GRACE as well as satellite and airplane based altimetry, finding negative acceleration in the ice mass signal over the last decade (Harig & Simons, 2016; Khan et al., 2015). Rates of ice loss increase by a combination of greater discharge from calving glacier termini at the edges of the ice-sheet as well as decreased surface mass-balance, the difference between seasonal snow accumulation and melting (Enderlin et al., 2014; Khan et al., 2015). Significant inter-annual variability and a-synchronicity have been observed in the discharge rates of the Greenland ice-sheet's major drainage basins, while surface mass-balance is comparatively more predictable (Enderlin et al., 2014; McMillan et al., 2016). Both contributions to ice loss were accelerating between 2000–2012, combining for a total acceleration of ice mass estimated around -30 Gt per year^2 over all of Greenland (Enderlin et al., 2014; Velicogna, 2009).

A recent study by Harig & Simons (2016) modeling the mass of the Greenland ice-sheet using GRACE data products showed deviations from the long-term quadratic trend, starting with a high level of mass loss in the summer of 2012 and followed by two summers of little mass loss in 2013 and 2014 (see Figure 1, adapted from Harig & Simons, 2016, their Figure 4). These deviations have been connected to atmospheric forcing from the North Atlantic Oscillation (NAO) suggesting that the changes from the expected mass balance were driven by summer surface mass balance as opposed to terminus discharge rate (McMillan et al., 2016).

Two and a half years later, and following the final season of the GRACE mission, we revisit the GRACE dataset using similar methods to Harig & Simons (2016) to analyze the continued signal of Greenland ice-sheet mass and investigate the relationship between surface mass-balance, the NAO, and inter-annual variability.

We show that previously fit quadratic trends do not describe the Greenland mass signal over the full GRACE time-period, and instead fit a linear model estimating the ice loss trend at approximately -239 ± 6 Gt per year. The 2013–2014 deviation, as well as larger structures present within the residuals of our linear model are compared to filtered time-series of the NAO index, and support irregular atmospheric forcings as a potential explanation.

Data and Methods

Methods of GRACE Data Reduction

The Gravity Recovery and Climate Experiment is a twin-satellite mission active 2002–2017, with its final data collection completed in October 2017. GRACE measurements are made accessible in the form of several data products offered through NASA and partnered agencies, which generally rely on a method of data reduction to translate the "Level 1" GRACE measurements of satellite positions into globally projected mass anomaly estimations. There are two primary methods of data reduction: The creation of "mascons", roughly equal-area sections around the globe on the scale of single arc-degrees, each assigned a single number representing mass change, and the calculation of spherical harmonic coefficients, which correspond to continuous functions in three dimensions that when summed can model the spatially continuous variation of mass on the surface of Earth.

The spherical harmonic method requires continuous functions on Earth's surface, whereby a field of interest can be developed into a series solution of eigenfunctions $Y_{lm}(\theta,\phi)$, where l refers to the "order" (integers 0 to ∞) and m the "degree" (integers $-l$ to $+l$) of each harmonic (θ and ϕ reference location on the surface of Earth). Due to limitations in computational power and in the spatial resolution of the data being modeled by the harmonic functions, calculated solutions are bandlimited, meaning that they are calculated up to a finite order L. See Simons et al. (2006), their section 3 for a concise summary. See our Figure 2 for illustrations of low-order spherical harmonic eigenfunctions.

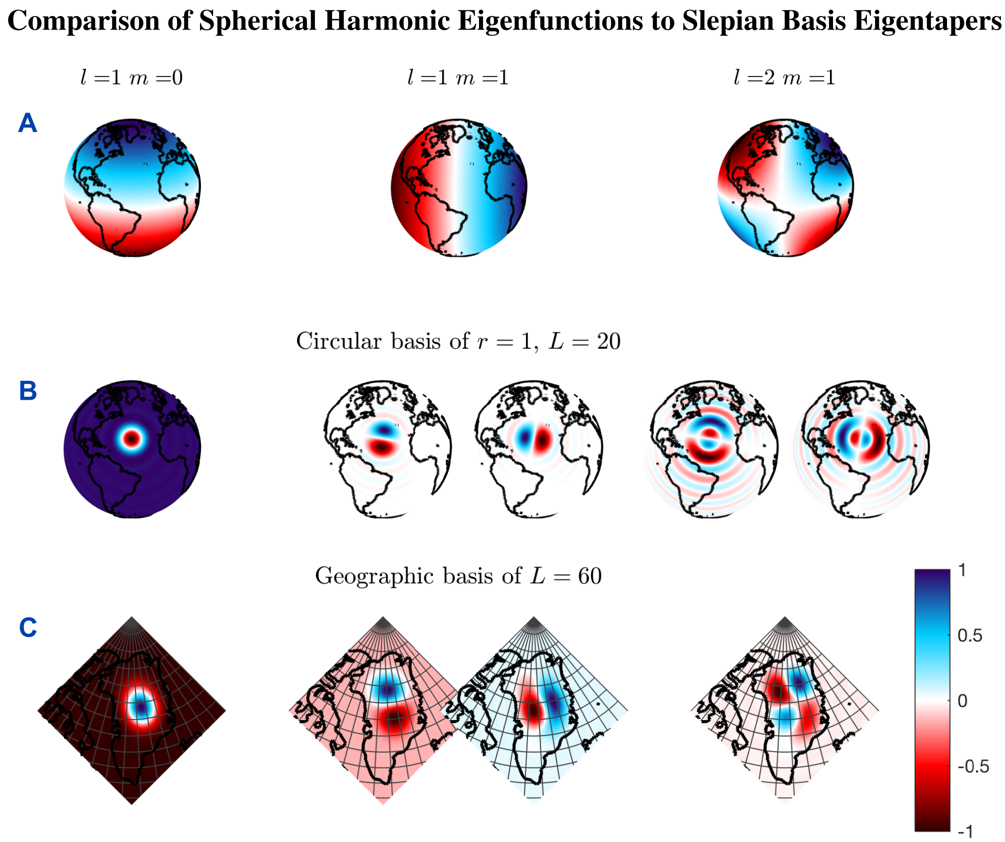

Figure 2: Three low-order spherical harmonic eigenfunctions $Y_{lm}(\theta,\phi)$ are illustrated in **A** as examples of the basic forms these functions take: zonal (left, $m = 0$), sectoral (middle, $m = l$), and tesseral (right, $m \neq l \neq 0$). When expanded into a geographically-localized Slepian basis, the forms of these eigenfunctions have parallel eigentapers as illustrated in rows **B** and **C**. The eigentapers allow for reconstruction of a signal with power concentrated within a geographical basis, minimizing the effect of the signal outside of the basis on the series solution. r is radius, L is the bandlimit of maximum order l used in the Slepian expansion (see Data and Methods: Methods of GRACE Data Reduction).

Monthly coefficients for bandlimited global spherical harmonic solutions of the time-variable geopotential field are independently calculated by three different processing centers (GFZ in Potsdam, Germany; CSR at University of Texas, Austin; JPL at California Institute of Technology) and published publicly as the GRACE Level 2 Release 05 products for a few different bandwidths (see Appendix A). The RL05 product is pre-corrected to remove the time-invariant geopotential field using the GRACE Gravity Model 03 (Tapley et al., 2007), and we use coefficients describing Earth's center of mass (spherical harmonic degree 1, from Swenson et al., 2008) and oblateness (spherical harmonic degree 2, order 0, from Cheng et al., 2013) calculated from Satellite Laser Ranging in order to accurately capture mass variations on scales much larger than the area covered by the GRACE satellites (see Appendix A). The coefficients are released as contributions to gravitational potential in units of $\frac{kg^2}{s^2}$, and are converted to equivalent surface density on Earth in units of $\frac{kg}{m^2}$ using the method of Wahr et al. (1998). Mass estimates are calculated through area-integration, and converted to sea-level equivalence using the method of Tian et al. (2015).

A third method of data reduction uses the spherical harmonic coefficients in a linear combination of their respective functions to constrain explanatory power to an arbitrary geographic location (Simons et al., 2006). This method generates linear combinations of the spherical harmonic eigenfunctions $Y_{lm}(\theta,\phi)$ called scalar Slepian functions $g_\alpha(\theta,\phi)$, where α refers to the "rank" of the Slepian function, which is a single linear combination of all spherical harmonic eigenfunctions up to order L, also referred to as an "eigentaper." Formally, this expansion is expressed in terms of the spherical harmonic eigenfunctions by:

$$\sum_{l=0}^{L}\sum_{m=-l}^{l} f_{lm}Y_{lm}(\theta,\phi) = \sum_{\alpha=1}^{(L+1)^2} f_\alpha g_\alpha(\theta,\phi)$$

By construction the functions $g_\alpha(\theta,\phi)$ are centered around the geographic region of interest. A few eigentapers are concentrated in power strictly within the region, and most are concentrated in power predominantly outside of the region. The signal within the region is approximated by choosing those functions $g_\alpha(\theta,\phi)$ whose ratio of power inside of that region to outside of the region is significant (often around $\geq \frac{1}{2}$), the number of which is referred to as the Shannon number N. The resulting spatially concentrated estimation of the global field is expressed in the approximation:

$$\sum_{l=0}^{L}\sum_{m=-l}^{l} f_{lm}Y_{lm}(\theta,\phi) \approx \sum_{\alpha=1}^{N} f_\alpha g_\alpha(\theta,\phi)$$

Though limited by N, the Slepian expansion is useful by reducing the unnecessary information in the global spherical harmonic coefficients — namely, the signal everywhere else in the world. The method of calculating geographically constrained scalar Slepian functions from a bandlimited series of spherical harmonics, as well as the relationship between the geographical area and the Shannon number is described in mathematical detail by Simons et al. (2006). See our Figure 2 for illustrations of low rank Slepian eigentapers in an circular, axisymmetric basis and a Greenland basis.

Slepian-based harmonics have the advantage of continuous solutions as opposed to the coarse rasterized solutions of mascons, with less of the noise and bias associated with globally continuous spherical harmonics. The expansion of global spherical harmonics into a localized Slepian basis of eigentapers allows for locally constrained signals to be extracted from the continuous global GRACE RL05 data product with less impact from noise or signals from other geographic locations, a problem that reduces the precision of the standard spherical harmonic method. We will find localized mass anomaly solutions using the Slepian expansion method of data reduction from the GRACE CSR RL05 $L = 60$ spherical harmonic coefficients (see Harig & Simons, 2012).

Our project builds upon the methods, results, and unresolved questions from previous work done by Chris Harig in the Simons Research Group in the Princeton Department of Geosciences. That work first applied the spherical Slepian basis to the analysis of Greenland ice mass, with results of lower error in both mass estimation and spatial distribution of the geopotential signal than previous studies using different analysis techniques (Harig & Simons, 2012).

The major data analysis of this project involves data manipulation and solution modeling in computer code. MATLAB code for the expansion of spherical harmonic eigenfunctions into Slepian bases and supplementary files are borrowed and adapted from publicly available code published through the Community Surface Dynamics Modeling System (see Appendix A).

General GRACE Examples

In the standard spherical harmonic basis, GRACE measurements are used to model surface density anomaly on a continuous global scale, as illustrated in Figure 3. Changes in surface density can be modeled as the difference in spherical harmonic coefficients between two dates. Difference maps clearly highlight seasonal changes in mass distribution such as the hydrologic cycles of temperate climates, as illustrated in Figures 4.

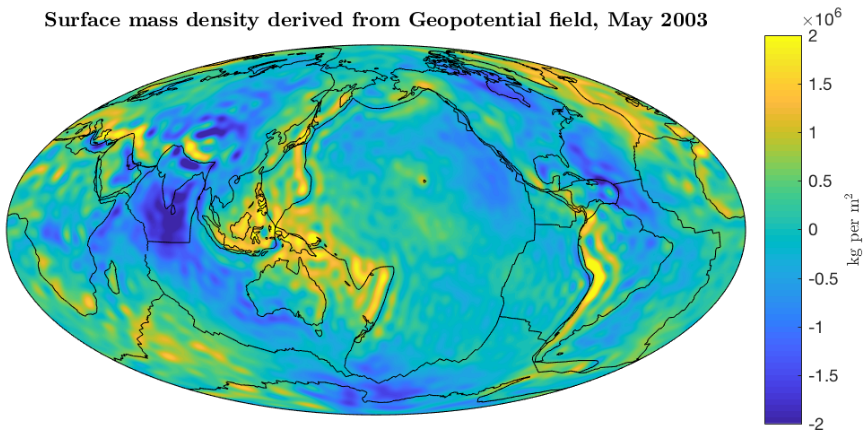

Figure 3: An example of Earth's time-variant surface density from the GRACE RL05 spherical harmonic coefficients, with corrected degrees 1 and 2 (see Data and Methods: Methods of GRACE Data Reduction). Note that the time-invariant signal has been removed (as per Tapley et al., 2007) revealing smaller scale features of Earth's mass distribution.

At smaller scales of mass change such as difference maps of the spherical harmonic coefficients, strong striping patterns are revealed that do not represent physically observed mass changes (Swenson & Wahr, 2006). This striping is commonly eliminated with a filter, blurring the stripes with data from nearby or with other spherical harmonic coefficients, the visual effect of which can be seen in Figure 4. However as the stripes are an artifact of sampling and are not random noise, we do not corrupt the signal with filtering or smoothing before expansion into a Slepian basis.

The Slepian Basis

Slepian expansion is comparable to other eigenvalue series solutions, with the approximation being valid within the basis, and with some small amount of residual (see Figure 5). The structure of these residuals appears to be periodic, and, similar to the Gibbs phenomenon in two dimensions, is an artifact of band-limitation. In order to fully capture the geographical edges of the

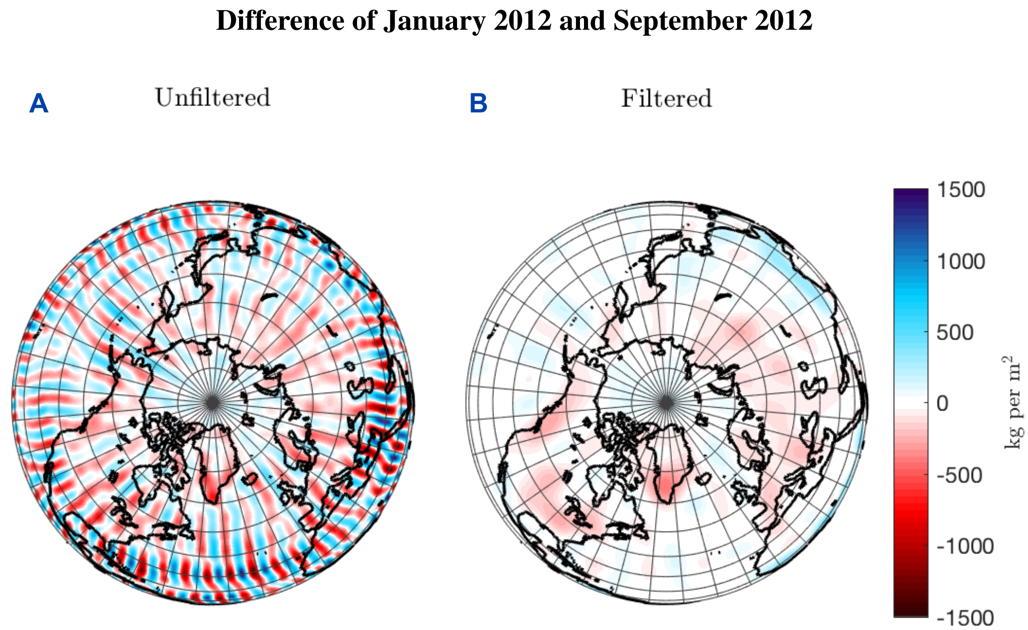

Figure 4: Difference maps illustrating the seasonal signals in global mass distribution for the season of greatest ice loss on Greenland over the GRACE period. Note the gain in mass in areas with strong summer wet seasons such as Southeast Asia, and the loss in mass in areas with summer snow-melt seasons such as Greenland. Note also the strong vertical striping characteristic of the spherical harmonic GRACE solutions in **A**. Shown in **B** are "de-striped" solutions, which use a filter to smooth away visible striping – a common approach. We avoid potentially filtering away signal, and instead use Slepian localization to improve the modeling of the unfiltered signal. See Figure 5 for comparison to our Slepian expansion.

basis while minimizing signal from outside, a buffer of $0.5°$ was chosen for the $L = 60$ GRACE data based on the results of Harig & Simons (2012) (see their Figure S6).

After localizing the signal into the Greenland Slepian basis, with the reduction of dimensionality from $L = 60$ to $N = 20$ that follows, we fit each time-variant Slepian coefficient f_α individually with polynomial (up to degree 3) and periodic (annual and semi-annual) functions using the method of Harig & Simons (2016) to produce a model of the expected seasonal signal within the Slepian basis (see Figure 8). We call this model the f_α model, in contrast to our linear models of the total signal of Greenland mass, which we will denote as $\underline{m}_1$ and $\underline{m}_2$ for 1^{st} and 2^{nd} degree unweighted polynomial models respectively. Uncertainty in the GRACE measurements are

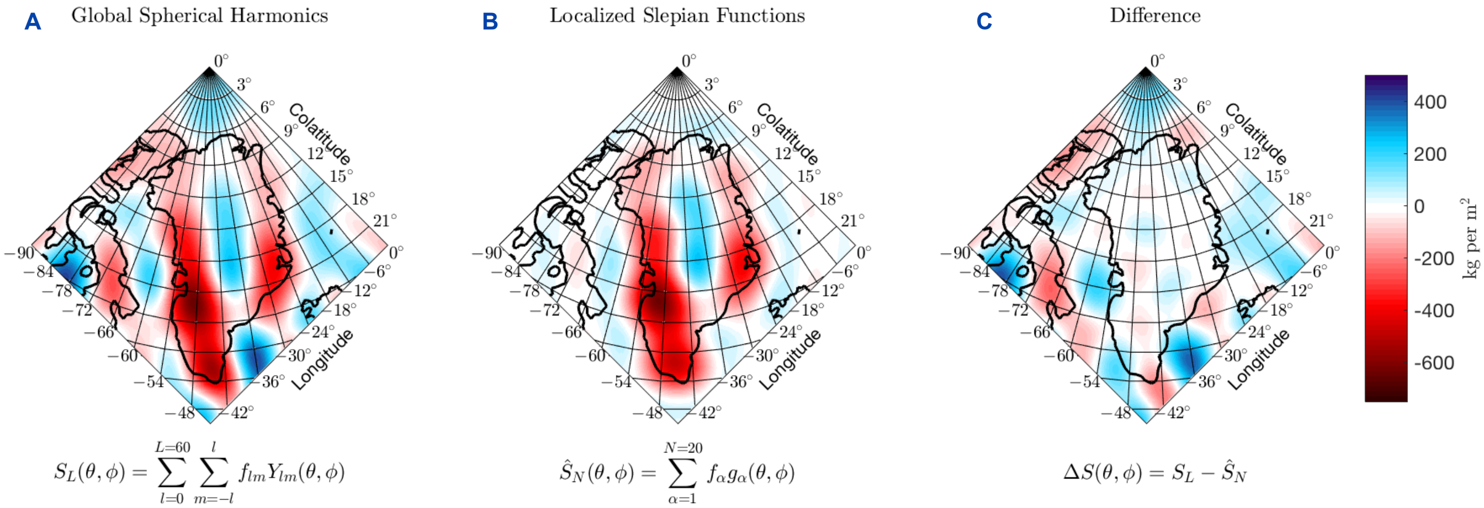

Figure 5: Maps of the difference between January 2012 and September 2012 as in Figure 4, illustrating the differences between the Spherical Harmonic and Slepian Expansions for $L = 60$ with a Greenland basis buffered by $0.5°$. Note the recovery of the signal compared to the filtered solution shown in Figure 4, and that the pattern of the residuals contains elements of the unwanted vertical striping as well as Gibbs-like harmonic patterns.

North Atlantic Oscillation Data

The North Atlantic Oscillation (NAO) is a the atmospheric oscillation of two high and low pressure centers in the North Atlantic Ocean, and the sea-level atmospheric pressure difference between those centers is used as a climate index that is strongly related to temperature, precipitation, and wind patterns across the North Atlantic (Hanna & Cropper, 2017). Past studies suggest correlation of high NAO indices with increased melting of Greenland ice, and lower NAO indices with increased accumulation of Greenland ice (McMillan et al., 2016). We use monthly NAO data published by the National Oceanic and Atmospheric Association filtered with a 6-month moving average and a 3-year moving average and compare these to the residuals of our Greenland mass models (see Figure 7 and Appendix A). We chose these windows to estimate the cumulative effects of the NAO over the approximate time-scale of variations in the model residuals.

Results

We found that between January, 2003 and June, 2017 the Greenland mass signal is best fit by our $\underline{m}_1$ linear model, with a slope of -238 ± 6 Gt per year, equivalent to approximately -0.66 ± 0.02 mm sea level per year, reflecting 95% confidence bounds on our model parameters (see Figure 6, B). Fitting with an $\underline{m}_2$ linear model returned an estimated acceleration of only -2.52 ± 0.38 Gt per year^2. We compared the relative performance of the $\underline{m}_1$ and $\underline{m}_2$ models by calculating the "explained variance" R^2 in the data d as:

$$\mathrm{R}^2 = 1 - \frac{\mathrm{var}(\underline{d} - \underline{m})}{\mathrm{var}(\underline{d})}$$

We found a reduction in R^2 of $\underline{m}_2$ compared to $\underline{m}_1$, leading us to reject the quadratic model $\underline{m}_2$ in favor of the first order polynomial model $\underline{m}_1$ as a better description of the 2003–2017 time-period. The $\underline{m}_1$ linear model was not significantly different between the previously analysed record (01/2003–06/2013) and the complete GRACE record (01/2003–06/2017), further supporting the use of $\underline{m}_1$ for the entire period, and suggesting that the years 2012–2014 were not a significant change-point in mass trend (see Figure 6, A).

The f_α model for the complete 2003–2017 GRACE record revealed deviations of over 2σ (as calculated from the propagated variance of each Slepian coefficient) in the expected seasonal trend (positive from 2009–2010 and negative from 2012–2013) also seen in the $\underline{m}_1$ residuals (see Figures 8 & 7.

Discussion

Our $\underline{m}_1$ trend of -238.91 ± 6.26 Gt per year calculated from the complete 2003–2017 GRACE record using Slepian functions is less than recent results from van den Broeke et al. (2016) who found a linear trend of -270 ± 4 Gt per year using the 2003–2015 GRACE record in standard spherical harmonics, and a trend of -294 ± 5 Gt per year using independent estimates of surface mass-balance and discharge, with the real uncertainty of their rates estimated at 20 Gt per year.

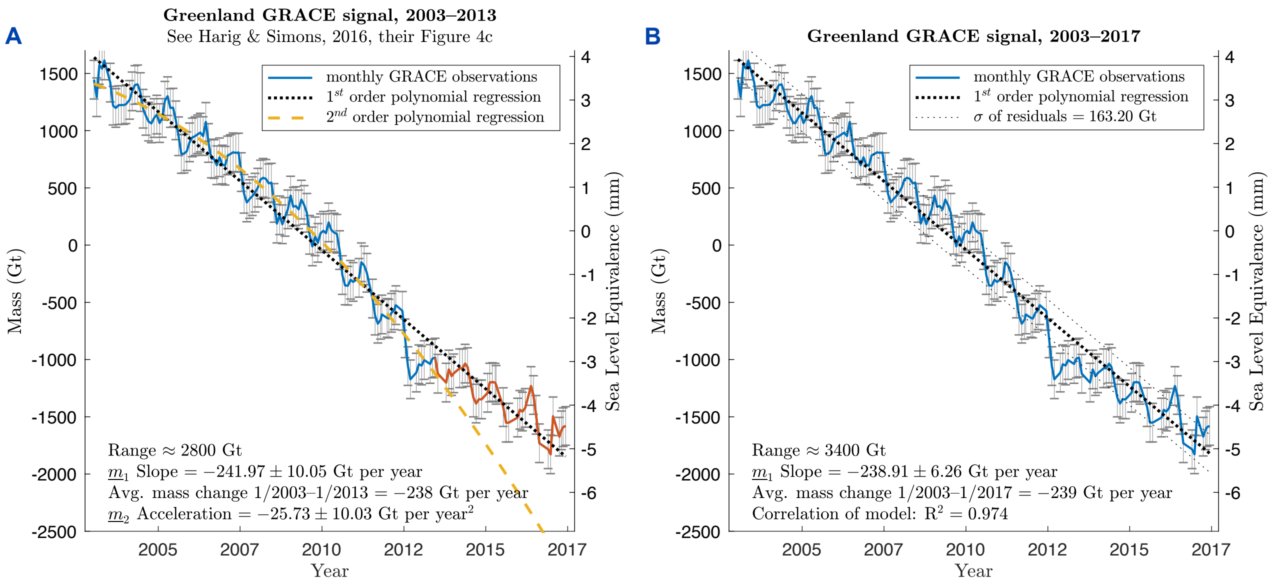

Figure 6: Total mass changes for Greenland over the complete GRACE record calculated using CSR RL05 $L = 60$ spherical harmonic coefficients and a 0.5° buffered Slepian basis (see Data and Methods: The Slepian Basis). Shown in **A** are the $\underline{m}_1$ and $\underline{m}_2$ linear models for 01/2003–06/2013, comparable to previous estimates of the mass trend (see Figure 1). Note the significant departure of the extrapolated $\underline{m}_2$ model from the continuing signal. Shown in **B** is the $\underline{m}_1$ linear model for 01/2003–06/2017 with the standard of deviation of its residuals. Note that the $\underline{m}_1$ model does not significantly change after including the entire GRACE record. Error-bars represent 2σ based on the combined variance of Slepian coefficients f_α.

Using the same GRACE record as van den Broeke et al. (2016), we still find a rate of only -245.34 ± 7.34 Gt per year.

The apparent anomaly of 2013–2014 observed by Harig & Simons (2016) was in fact a combination of the season of greatest ice-loss on record in the summer of 2012 (see Figures 4 & 5) followed by the season of least ice loss on record in the summer of 2013 (see Figure 6). With our linear estimate of the long-term trend we can re-adjust our expectations of the Greenland mass signal to see that the combination of these two years effectively canceled each other out, suggesting that intense melting years and low melting years may commonly occur within the long-term record. In comparing our f_α model (Figure 8, A) to that of Harig & Simons (2016) (Figure 1), we see the same shift from quadratic to linear trend, as well as the clarification of anomalous years — more ice than expected in 2009–2010, less ice than expected in 2012–2013 (Figure 8, B). The significant anomalies seen in these years suggest that inter-annual variability is forced by irregular signals not captured in our f_α model.

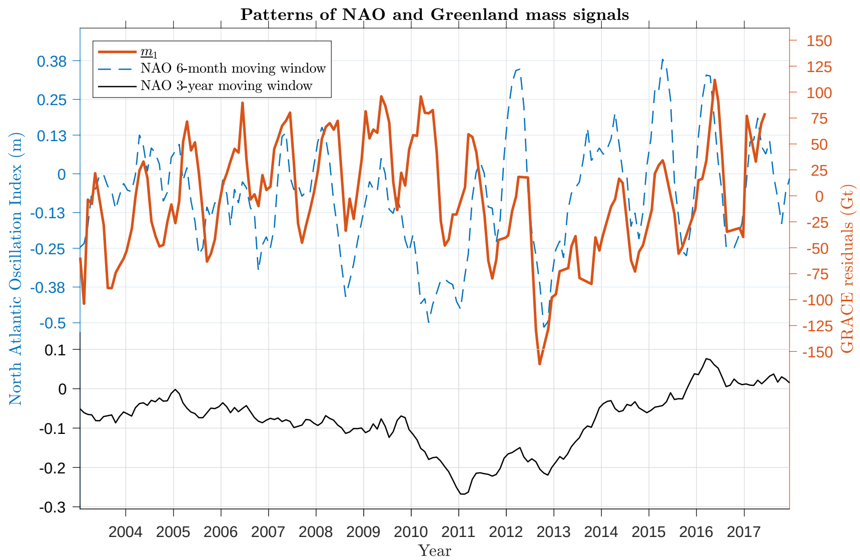

Figure 7: Residuals from our $\underline{m}_1$ model of the Greenland mass signal compared to 6-month and 3-year moving averages of the NAO index (see Data and Methods: North Atlantic Oscillation Data). On top, note the seasonal rising and falling of the Greenland ice-sheet mass in the model residual, and that it is correlated with the 6-month NAO signal especially from 2012 onwards. The steep drop in ice mass in 2012 that marked the beginning of the 2013–2014 anomaly coincided with a steep drop between two extremes of the NAO index, while the little melt in 2013 coincided with a sustained high NAO index that summer. On bottom, notice the decline of the 3-year NAO index from 2005–2011, and its general rise from 2013–2017. These long-term signals are coincident with the general long-term structure of the residuals as well.

Inter-annual variability within the Greenland mass signal is discussed by McMillan et al. (2016), who note the correlation between the 2012–2013 anomalies and the North Atlantic Oscillation (NAO). We find related patterns in comparing our $\underline{m}_1$ residuals to the NAO, with strong negative phases generally aligned with greater melting, and strong positive phases generally aligned with greater accumulation both on seasonal and multi-year time-scales (see Figure 7). Interestingly, the NAO signal becomes more closely correlated with the Greenland mass signal starting in 2012, which aligns with studies suggesting that atmospheric forcing has become an increasingly important driver of the Greenland ice-sheet compared to discharge over the last decade (Enderlin et al., 2014). The positive deviations in 2009–2010 do not appear related to the NAO, making it clear that other forcing signals remain unaccounted for. While the effect of atmospheric forcing such as the NAO upon the Greenland ice-sheet is apparent, the long-term unpredictability of the the NAO as well as the feedback between ice and atmosphere make it

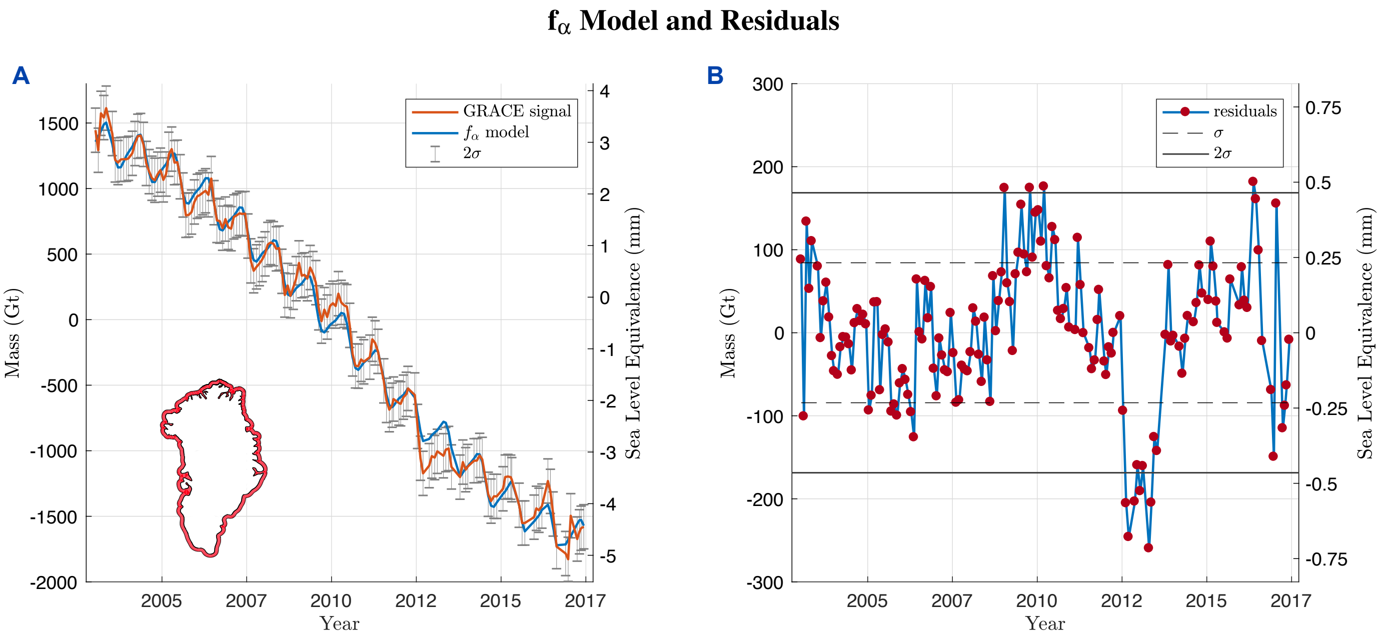

Figure 8: A comparison of the 2003–2017 Greenland mass signal from GRACE with the f_α model of linear and seasonal trends in the Slepian coefficients (see Data and Methods: The Slepian Basis). **A** are the time-series for both the signal and the model, and **B** are the residuals. 2σ refers to two standards-of-deviation based on the propagated variance of each Slepian coefficient, and represents the best estimate of uncertainty in the Slepian GRACE solution (see Harig & Simons, 2012, their Supporting Information). Note the increase in deviations from the model as compared to the equivalent model by Harig & Simons (2016) seen in Figure 1, and the significant deviations in the de-trended time series in 2009–2010 and 2012–2013.

difficult to resolve the elements of the observed Greenland mass trend that are due to such noisy and transient weather patterns as opposed to long-term trends.

Conclusions

Using an $L = 60$, $0.5°$ buffered Slepian basis for Greenland to localize the GRACE mass signal for the Greenland ice-sheet, we found the best estimate for the ice loss over the 2003–2017 GRACE record to be -238.91 ± 6.26 Gt per year, equivalent to approximately 55 ± 1.5 mm of sea level rise by 2100. This rate is similar to past estimates with the exception that no significant acceleration was found for the entire time-period. Greenland was losing ice at increasing rates between 2003–2012, but based on our results negative acceleration may not be the expected long-term behavior of the signal. Our comparison of our model residuals to NAO atmospheric forcing suggests that deviations from the long-term trend may be caused by irregular atmospheric forcing on sub-annual and multi-year time-scales, making it difficult to determine which elements of the signal are trend as opposed to variability. We expect this work to be refined and improved upon with the anticipated release of the GRACE Level 2 RL06 coefficient solutions and the 2018 launch of the GRACE Follow-On mission that will extend the global time-variant geopotential dataset and allow for the continued gravimetric analysis of the Greenland ice-sheet.

Appendix A

RL05 spherical harmonic coefficients for the time-variant geopotential field from the GFZ, JPL, and CSR data processing centers are available at:

ftp://podaac.jpl.nasa.gov/allData/grace/L2/

Coefficients describing Earth's center of mass (spherical harmonic degree 1, from Swenson et al., 2008) are available at:

ftp://podaac-ftp.jpl.nasa.gov/GeodeticsGravity/tellus/L2/degree_1/

Coefficients describing Earth's oblateness (spherical harmonic degree 2, order 0, from Cheng et al., 2013) are available at:

ftp://ftp.csr.utexas.edu/pub/slr/degree_2/

MATLAB code for the expansion and of spherical harmonic eigenfunctions into Slepian bases and manipulation of GRACE files is borrowed and adapted from:

https://github.com/csdms-contrib/

Monthly values for the North Atlantic Oscillation Index are calculated by the Climate Prediction Center, with normalized monthly average values January 1950 available at:

http://www.cpc.ncep.noaa.gov/products/precip/CWlink/pna/nao_index.html

References

Cheng, M., Tapley, B. D., & Ries, J. C., 2013. Deceleration in the Earth's oblateness, *Journal of Geophysical Research: Solid Earth*, **118**(2), 740–747, doi: 10.1002/jgrb.50058.

Enderlin, E. M., Howat, I. M., Jeong, S., Noh, M.-J., van Angelen, J. H., & van den Broeke, M. R., 2014. An improved mass budget for the Greenland ice sheet, *Geophysical Research Letters*, **41**(3), 866–872 doi 10.1002/2013GL059010.

Hanna, E. & Cropper, T. E., 2017. *Oxford Research Encyclopedia, Climate Science*, chap. North Atlantic Oscillation, p. doi: 10.1093/acrefore/9780190228620.013.22, Oxford University Press.

Harig, C. & Simons, F. J., 2012. Mapping Greenland's mass loss in space and time, *Proc. Natl. Acad. Sc.*, **109**(49), 19934–19937, doi: 10.1073/pnas.1206785109.

Harig, C. & Simons, F. J., 2015. Accelerated West Antarctic ice mass loss continues to outpace East Antarctic gains, *Earth Planet. Sci. Lett.*, **415**, 134–141, doi: 10.1016/j.epsl.2015.01.029.

Harig, C. & Simons, F. J., 2016. Ice mass loss in Greenland, the Gulf of Alaska, and the Canadian Archipelago: Seasonal cycles and decadal trends, *Geophysical Research Letters*, **43**(7), 3150–3159.

Hartmann, D., Tank, A. K., Rusticucci, M., Alexander, L., Brönnimann, S., Charabi, Y., Dentener, F., Dlugokencky, E., Easterling, D., Kaplan, A., Soden, B., Thorne, P., Wild, M., & Zhai, P., 2013. *Climate Change 2013: The Physical Science Basis. Contribution of Working Group I Contribution to the Fifth Assessment Report of the Intergovernmental Panel on Climate Change*, chap. Observations: Atmosphere and Surface, p. doi: 10.1017/CBO9781107415324, Cambridge Univ. Press.

Khan, S. A., Aschwanden, A., Bjørk, A. A., Wahr, J., Kjeldsen, K. K., & Kjær, K. H., 2015. Greenland ice sheet mass balance: a review, *Reports on Progress in Physics*, **78**(4), 046801.

McMillan, M., Leeson, A., Shepherd, A., Briggs, K., Armitage, T. W., Hogg, A., Munneke, P. K., van den Broeke, M., Noël, B., van de Berg, W. J., Ligtenberg, S., Horwath, M., Groh, A., Muir, A., & Gilbert, L., 2016. A high-resolution record of Greenland mass balance, *Geophysical Research Letters*, **43**(13), 7002–7010.

Simons, F. J., Dahlen, F. A., & Wieczorek, M. A., 2006. Spatiospectral concentration on a sphere, *SIAM Rev.*, **48**(3), 504–536, doi: 10.1137/S0036144504445765.

Swenson, S. & Wahr, J., 2006. Post-processing removal of correlated errors in GRACE data, *Geophysical Research Letters*, **33**(8), doi: 10.1029/2005GL025285, L08402.

Swenson, S., Chambers, D., & Wahr, J., 2008. Estimating geocenter variations from a combination of GRACE and ocean model output, *Journal of Geophysical Research: Solid Earth*, **113**(B8), doi: 10.1029/2007JB005338.

Tapley, B. D., Ries, J. C., Bettadpur, S., Chambers, D., Cheng, M., Condi, F., & Poole, S., 2007. The GGM03 Mean Earth Gravity Model from GRACE, in *88(52), Fall Meet. Suppl.*, Abstract G42A-03, Eos Trans. AGU.

Tian, Y., Scaioni, M., Tong, X., & Li, R., 2015. On the Conversion of Antarctic Ice-Mass Change to Sea Level Equivalent, *Marine Geodesy*, **38**(1), 89–97, doi: 10.1080/01490419.2014.969458.

van den Broeke, M. R., Enderlin, E. M., Howat, I. M., No el, B. P., van de Berg, W. J., Meijgaard, E. v., & Wouters, B., 2016. On the recent contribution of the Greenland ice sheet to sea level change, *The Cryosphere*, **10**(5), 1933–1946, doi: doi:10.5194/tc–10–1933–2016, Copyright - Copyright Copernicus GmbH 2016; Last updated - 2016-10-01.

Vaughan, D., Comiso, J., Allison, I., Carrasco, J., Kaser, G., Kwok, R., Mote, P., Murray, T., Paul, F., Ren, J., Rignot, E., Solomina, O., Steffen, K., & Zhang, T., 2013. *Climate Change 2013: The Physical Science Basis. Contribution of Working Group I Contribution to the Fifth Assessment Report*, chap. Observations: Cryosphere, p. doi: 10.1017/CBO9781107415324, Cambridge Univ. Press.

Velicogna, I., 2009. Increasing rates of ice mass loss from the Greenland and Antarctic ice sheets revealed by GRACE, *Geophysical Research Letters*, **36**(19), doi 10.1029/2009GL040222, L19503.

Wahr, J., Molenaar, M., & Bryan, F., 1998. Time variability of the Earth's gravity field: Hydrological and oceanic effects and their possible detection using GRACE, *Journal of Geophysical Research: Solid Earth*, **103**(B12), 30205–30229.